

Nonharmonic phonons in MgB₂ at elevated temperatures

N. D. Markovskiy,¹ J. A. Muñoz,¹ M. S. Lucas,² Chen W. Li,¹ O. Delaire,² M. B. Stone,² D. L. Abernathy,² and B. Fultz¹

¹California Institute of Technology, Department of Applied Physics and Materials Science, Pasadena, California 91125, USA

²Oak Ridge National Laboratory, 1 Bethel Valley Road, Oak Ridge, Tennessee 37831, USA

(Received 21 November 2010; revised manuscript received 11 March 2011; published 4 May 2011)

Inelastic neutron scattering was used to measure phonon spectra in MgB₂ and Mg_{0.75}Al_{0.25}B₂ from 7 to 750 K to investigate anharmonicity and adiabatic electron-phonon coupling. First-principles calculations of phonons with a linear response method were performed at multiple unit cell volumes, and the Helmholtz free energy was minimized to obtain the lattice parameters and phonon dynamics at elevated temperature in the quasiharmonic approximation. Most of the temperature dependence of the phonon density of states could be understood with the quasiharmonic approximation, although there was also significant thermal broadening of the phonon spectra. In comparison to Mg_{0.75}Al_{0.25}B₂, in the energy range of 60 to 80 meV the experimental phonon spectra from MgB₂ showed a nonmonotonic change with temperature around 500 K. This may originate from a change with temperature of the adiabatic electron-phonon coupling.

DOI: [10.1103/PhysRevB.83.174301](https://doi.org/10.1103/PhysRevB.83.174301)

PACS number(s): 74.25.Kc, 78.70.Nx, 71.15.Mb, 74.70.Ad

I. INTRODUCTION

Superconductivity in magnesium diboride¹ (MgB₂) has attracted widespread attention. Phonon-mediated electron pairing was early suspected as the mechanism of superconductivity, although the superconducting transition temperature $T_c \approx 39$ K would be the highest known for this mechanism. Soon it was established that the superconductivity of MgB₂ has a two-band character and BCS-type electron pairing^{2–9} with unusually strong, anisotropic electron-phonon coupling.^{7–13} It was shown that electron states in the covalent σ band, originating with in-plane boron sp^2 hybridized orbitals, couple very strongly to the E_{2g} phonon mode with its in-plane B-B bond stretching.^{9,13,14}

Nevertheless, several aspects of superconductivity in MgB₂, including the importance of phonon anharmonicity, are not fully understood and remain controversial. First-principles calculations of the E_{2g} phonon frequency at Γ , based on the harmonic approximation, significantly underestimate numerous Raman spectroscopy measurements.^{15–21} Frozen-phonon calculations^{4,6,7,9,12,13,22,23} are in excellent agreement at 0 K, and thus this discrepancy has been attributed to the onset of anharmonicity. Anharmonicity could play a significant role in explaining the high T_c and small isotope effect.^{3,24} Later calculations, based on a more rigorous perturbation theory approach, showed that the effects of anharmonicity are much smaller, owing to a negative contribution of the three-phonon scattering term,^{20,23} in accord with more recent inelastic x-ray scattering and tunneling spectroscopy measurements.^{14,20,25,26} Today the thermal shifts and broadenings of Raman peaks have not yet been related to the phonon dynamics and await theoretical explanation.^{19–21,27–29}

Nonharmonic behavior is generally expected at high temperatures, and interesting thermodynamic effects can occur when temperature causes changes in the electron-phonon interaction (EPI) or phonon-phonon interaction. A phonon distorts a crystal, and the potential energy of this distortion can be considered all electronic in origin, but the kinetic energy of the phonon is in the motion of the nuclei. For a harmonic phonon, the EPI affects equally the energies

of the electrons and the phonons. The “adiabatic” EPI requires simultaneous thermal excitations of both electrons and phonons. The strong EPI of MgB₂ may affect its thermodynamics at high temperatures because the adiabatic EPI may be expected to change with temperature, much as was found for superconducting transition metals.^{30–32} To date, studies on the phonon dynamics^{9,14,15,17–21,25,26,33} and lattice expansion^{18,34–38} of MgB₂ have been limited to temperatures 300 K or below.

The electronic structure near the Fermi energy is sensitive to the lattice constants a and c , and to the amplitude of boron atom displacements.^{22,39} The anharmonicities of the E_{2g} phonon modes are affected by the positions of partially filled boron σ bands relative to the Fermi level.^{9,22} Substitution of Al for Mg lowers the critical temperature for superconductivity, and it was previously shown that the phonon density of states (DOS) of Mg_{1– x} Al _{x} B₂ is very sensitive to the concentration of Al.^{12,40} This was attributed to Al donating its $3p$ electrons to the sp^2 “hole pockets” of MgB₂. The filling of the hole pockets by Al doping is expected to affect the electronic screening of B atom displacements, altering the interatomic forces between B atoms. Another effect of Al doping should be to alter the temperature dependence of the EPI, since the thermal broadening of electron occupancies and the thermal lifetime broadening of electron levels will change with band filling. This should be reflected in differences in the temperature dependence of the phonon density of states.

Here we present results from experimental and computational work on MgB₂ at elevated temperatures. Neutron-weighted densities of states (NWDOSs) were obtained from inelastic neutron scattering (INS) spectra measured on MgB₂ and Mg_{0.75}Al_{0.25}B₂ to identify the effects of doping. *Ab initio* calculations were performed for MgB₂, MgAlB₄, and AlB₂, using the quasiharmonic (QH) approximation. The lattice dynamics of MgB₂ can be mostly understood with the QH approximation, but nonharmonic behavior is found for phonons in the energy region of the E_{2g} phonon modes of MgB₂.

II. EXPERIMENT

The samples were synthesized by direct reaction of turnings of 99.98% pure Mg, 99.5% pure Al powders of 325 mesh, and 100-mesh powders of 98.78% isotopically enriched ^{11}B . The elements were enclosed in tantalum cylinders with welded seals, and reacted for 1 h at 107 K and then for 2 h at 1223 K in quartz tubes under an argon atmosphere. The product was ground into a fine powder and annealed in the same way at 1223 K for 15 h. The sample was finally annealed under dynamic vacuum at 750 K for 8 h to remove any unreacted Mg. Rietveld refinement of the x-ray diffraction (XRD) patterns showed the materials to have phase purities of 95%, with the main impurity phases being MgB_4 (3%) and MgO (2%).

Inelastic neutron scattering measurements were performed with the wide angular-range chopper spectrometer (ARCS) of the Spallation Neutron Source (SNS) at the Oak Ridge National Laboratory. For all results reported here, about 10 g of MgB_2 or $\text{Mg}_{0.75}\text{Al}_{0.25}\text{B}_2$ powders were accommodated in an annular aluminum can with an outer diameter of 2.9 and an inner diameter of 2.7 cm, resulting in the scattering of about 10% of the incident neutron beam. The sample was mounted in either a closed-cycle helium refrigerator or a low-background resistive furnace with thin aluminum shielding for thermal radiation, and neutron-absorbing boron nitride to suppress extraneous scattering. The nominal incident energy for all measurements was 165 meV. The energy resolution [full width at half maximum (FWHM)] was 3.0 meV at 100 meV neutron energy loss, increasing to 7.2 meV at the elastic line. Neutron diffraction patterns, obtained by integrating the elastic part of the data (from -5 to 5 meV), gave lattice parameters in agreement with the literature and our XRD measurements, and showed no evidence of any phase transitions as a function of temperature.

The raw INS data were rebinned into intensity I as a function of momentum transfer Q and energy transfer E . Differences in efficiency between detectors were corrected with measurements on a vanadium rod. Neutron-weighted phonon densities of states curves were calculated from $I(Q, E)$ in the incoherent scattering approximation. The measured background was subtracted and an iterative procedure was used to remove contributions from multiple scattering and higher-order multiphonon processes.^{41,42} The analysis includes corrections for Bose-Einstein and Debye-Waller factors. The neutron weights for phonon scattering are the ratios of neutron cross section to mass, σ/M , which are 0.153 and 0.534 barns/amu for Mg and B, respectively, so the motions of B atoms are overemphasized by a 7:1 ratio for MgB_2 . Results are shown in Figs. 1 and 2.

III. COMPUTATIONS

Electronic structure calculations⁴³ were performed with density functional theory (DFT) in the generalized gradient approximation.⁴⁴ For computationally feasible energy cutoffs, all calculations used ultrasoft⁴⁵ pseudopotentials for B and norm-conserving pseudopotentials⁴⁶ for Mg and Al. An energy cutoff of 64 Ry was used in the plane wave expansion and a charge density cutoff of 256 Ry with Monkhorst-Pack⁴⁷ $32 \times 32 \times 32$ k -point grids for MgB_2 and AlB_2 , and

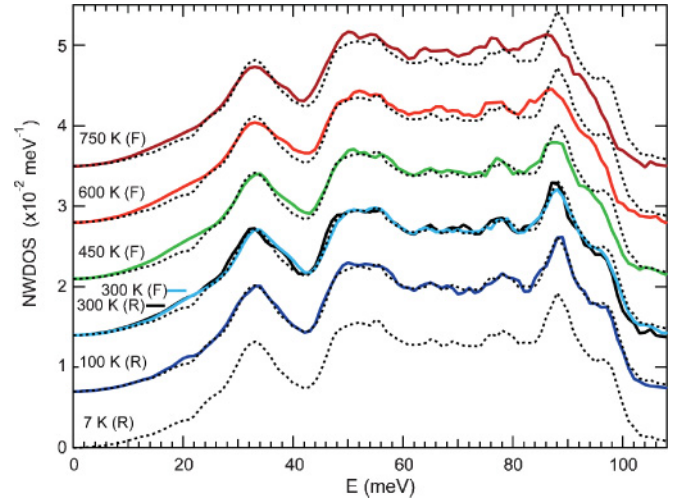


FIG. 1. (Color online) Neutron-weighted phonon DOSs of MgB_2 from INS data measured at temperatures as labeled, with sample in furnace (F) or refrigerator (R). Dotted lines, next to the higher-temperature curves, correspond to the 7 K result, shifted vertically by a constant.

$32 \times 32 \times 16$ for MgAlB_4 . A Methfessel-Paxton⁴⁸ smearing of 0.015 Ry for Brillouin zone integration was used to ensure adequate convergence of energy and phonon frequencies for free-energy minimization in the quasiharmonic model. The phonon calculations were performed on relaxed structures. The lattice parameters obtained for MgB_2 , MgAlB_4 , and AlB_2 were $a = 3.063$ Å and $c = 3.482$ Å, $a = 3.030$ Å and $c = 6.694$ Å, $a = 3.001$ Å and $c = 3.273$ Å, respectively, in good agreement with experimental results.^{34,35,49,50} Phonon frequencies and eigenmodes were calculated using the linear response technique.⁵¹ The dynamical matrices for calculations on fine meshes were obtained from a Fourier interpolation of the dynamical matrices computed on $6 \times 6 \times 6$ phonon

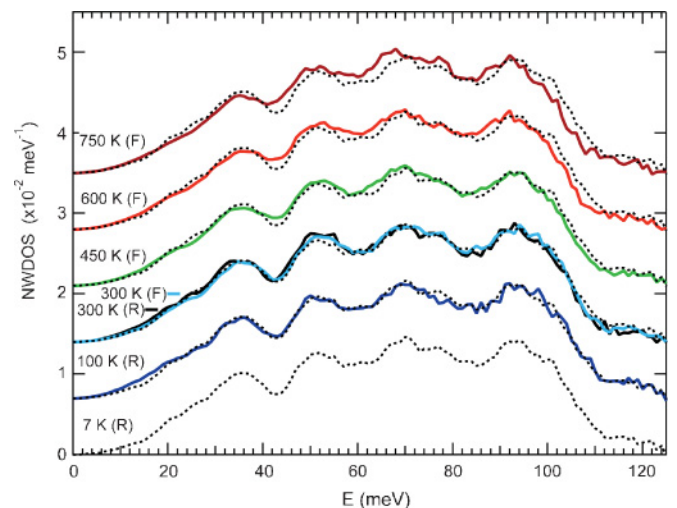


FIG. 2. (Color online) Neutron-weighted phonon DOSs of $\text{Mg}_{0.75}\text{Al}_{0.25}\text{B}_2$ from INS data measured at temperatures as labeled, with sample in furnace (F) or refrigerator (R). Dotted lines, next to the higher temperature curves, correspond to the 7 K result, shifted vertically by a constant.

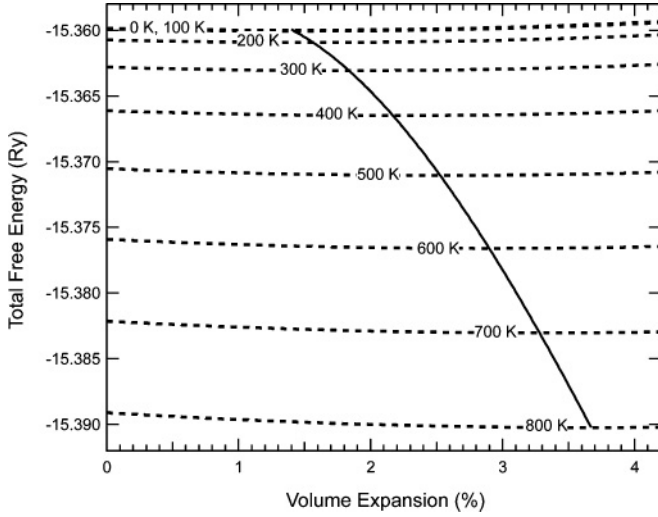


FIG. 3. Computed Helmholtz free energy (total, electronic plus phonon) as a function of volume expansion. Line crossings show energy minima at different temperatures.

meshes. Phonon densities of states then were computed on $28 \times 28 \times 28$ meshes using the tetrahedron scheme.

To calculate the effects of thermal expansion on phonons, we used the quasiharmonic approximation. The QH approximation assumes phonons to be harmonic, and effects of nonharmonicity enter through the volume dependence. Quasiharmonicity may be the major contributor to many thermodynamic properties at elevated temperatures, if the theoretical model is of sufficient quality.⁵² We performed a series of calculations at increasing volumes. At each volume, the lattice parameters a and c and the atomic positions in the unit cell were independently optimized to minimize the electronic energy $U_{el}(V)$, which was then fitted using the Birch-Murnaghan equation of state. Phonon free energies were computed from the calculated phonon DOS using the harmonic approximation,

$$F_{\text{ph}}(T, V) = \int \left[\frac{\hbar\omega}{2} + k_{\text{B}}T \ln(1 - e^{-\hbar\omega/k_{\text{B}}T}) \right] g_V(\omega) d\omega, \quad (1)$$

where $g_V(\omega)$ is a phonon DOS from a DFT linear response calculation at a specific volume. At each temperature, the free energy of Eq. (1) was fitted to a polynomial in V , and the minimum value of the Helmholtz free energy, $F_{\text{tot}}(T, V) = U_{el}(V) + F_{\text{ph}}(T, V)$, was used to obtain the optimal volumes and lattice parameters at fixed temperatures as shown in Fig. 3. Note the substantial effect from the zero-point energy.

IV. RESULTS

Figure 4 presents the thermal expansion $\Delta a/a_0$ and $\Delta c/c_0$ of MgB₂ from calculations in the QH approximation, and from experiment. Our experimental data, obtained from 325 to 898 K, match well with prior results from lower temperatures.^{34,35} Our lattice parameters at room temperature were $a_{\text{RT}} = 3.0856 \text{ \AA}$ and $c_{\text{RT}} = 3.5239 \text{ \AA}$, in good agreement with $a_{297\text{K}} = 3.08489 \text{ \AA}$ from Ref. 34 and $c_{\text{RT}} = 3.52196 \text{ \AA}$ from Ref. 35. The calculated thermal expansions are in

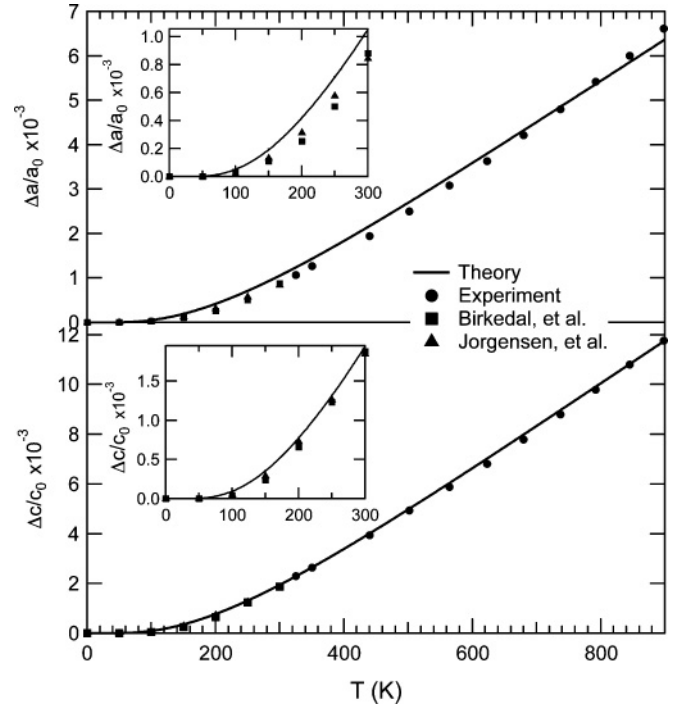


FIG. 4. Linear thermal expansion $\Delta L/L_{0\text{K}}$ of MgB₂ in the QH approximation for the a (upper) and c (lower) axes, in comparison with the present experiment and earlier reports (Refs. 34 and 35). Insets enlarge the low-temperature region.

good agreement with experiment to 900 K and, as in earlier reports,^{18,34–38} are about twice as large along c as along a .

The neutron-weighted phonon densities of states of MgB₂ and Mg_{0.75}Al_{0.25}B₂ (Figs. 1 and 2) from measurements with samples in the closed-cycle refrigerator at 7, 100, and 300 K are very similar, and show the small variability of the experimental results. There were some differences in background between the spectra from measurements in the refrigerator at 300 K and in the furnace at 300 K, but the changes in spectra from the furnace measurements can be identified reliably. For measurements at 300 K and below, the NWDOSs are in good agreement with published results.^{9,33,40} At 600 and 750 K the NWDOS curves broaden noticeably in the energy region of 60–95 meV, and the high-energy peak softens considerably.

A set of NWDOS curves were obtained as follows from the first-principles calculations. The calculated phonon partial DOS curves of the individual elements were multiplied by appropriate neutron weighting factors and summed. Next, they were convolved with an energy-dependent experimental resolution function characteristic of the ARCS spectrometer. The calculated NWDOS curves are shown in Fig. 5. The thermal trends are generally consistent with our experimental results from Fig. 1, although thermal broadening does not occur in the QH approximation, and broadening from the zero-point motions is also missing. The thermal shifts for the QH NWDOSs calculated for MgAlB₄ were similar, although a bit smaller.

The experimental NWDOS curves of MgB₂ and Mg_{0.75}Al_{0.25}B₂ (Figs. 1 and 2) were analyzed with a simple model that assumes all phonons shift in energy quasiharmonically with one Grüneisen parameter γ and broaden with

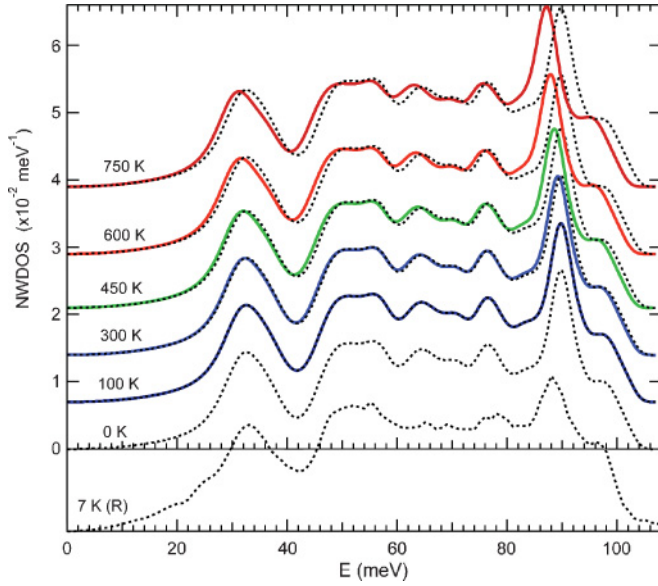


FIG. 5. (Color online) Temperature dependence of computed NWDOSs of MgB₂ in the QH approximation. Curve appended at bottom is an experimental curve from Fig. 1. Dotted lines, next to the higher-temperature curves, correspond to the 7 K result, shifted by a constant.

temperature as damped harmonic oscillators $D(Q, E', E)$ with a single quality factor Q .^{41,42} To get each high-temperature NWDOS, g_T , the experimental NWDOS curve obtained at 7 K was rescaled in energy through γ , and convolved with a Lorentzian with half width at half maximum $\Gamma = \omega/2Q$ at each energy: $g_T(E) = D(Q, E', E) * g_{7K}[(1 + \gamma)E']$, and renormalized. The parameters γ and Q were optimized for best fits to the NWDOS curves at higher temperatures. The procedure was generally successful, as shown by the results of Fig. 6 for MgB₂, which includes the modeled and actual differences between the NWDOS curves at 7 and 750 K. Also shown is the difference between the *ab initio* quasiharmonic results for the same temperatures. The two quasiharmonic approaches are in reasonable agreement with each other, although the sharper features in the *ab initio* NWDOS curves give large difference peaks from 80 to 95 meV. The experimental difference of NWDOS curves of MgB₂ shows some differences, including a broad difference over the energy range from 50 to 80 meV. Figure 7 shows the difference between the differential experimental and theoretical NWDOS curves, $\Delta[\Delta\text{NWDOS}(T)] = \Delta\text{NWDOS}_{\text{expt}}(T) - \Delta\text{NWDOS}_{\text{theor}}(T)$, at different temperatures. Overall, there is a good correspondence, and no significant shifts throughout the energy range. The plot displays some changes of shape with temperature in the 50 to 80 meV region, and noticeable shifting around 84 meV, caused by the asymmetrical broadening of the corresponding experimental peak (Fig. 1).

Computed dispersions of phonons and Grüneisen parameters for MgB₂ are presented in Fig. 8. The phonon dispersions are in good agreement with previous work.^{15,23} The Grüneisen parameters were obtained by fitting phonon frequencies obtained at 0 K for a series of volume expansions up to 0.1% from equilibrium: $(\omega/\omega_0 - 1) = -\gamma(V/V_0 - 1) + \chi(V/V_0 - 1)^2 + \dots$. The calculated Grüneisen parameters

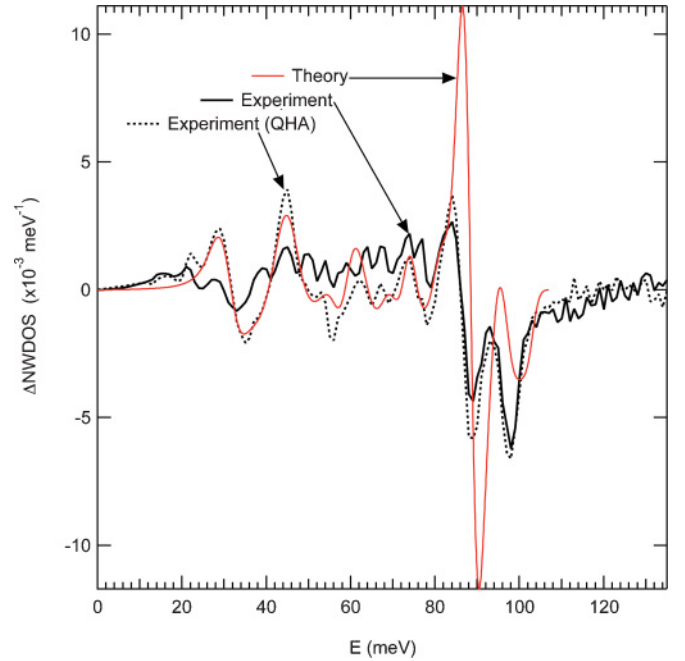


FIG. 6. (Color online) Differences of NWDOS curves of MgB₂ at 7 and 750 K. “Experiment” is from actual NWDOS curves, “Experiment (QHA)” is from the difference using a 750 K curve from two-parameter modification of the 7 K experimental data (see text), and “Theory” is the difference between the curves computed by *ab initio* QH theory. The experimental curves were corrected for the differences between the spectra acquired from samples in the furnace and refrigerator at 300 K.

(Fig. 8) are all positive, but highly anisotropic. Our calculations of dispersions along the Γ -A direction for three compounds of different Al concentrations are presented in Fig. 9. The phonon frequencies, especially of E_{2g} modes, are very sensitive to the Al concentration in Mg-rich material, as was pointed out earlier.⁴⁰ In comparison to AlB₂ and MgAlB₄, the E_{2g} modes of MgB₂ along the Γ -A direction have low frequencies and large Grüneisen parameters. Nevertheless, other modes contribute to the NWDOS in the energy range from 60 to 80 meV, and the net effect of this large quasiharmonic phonon softening in Fig. 5 is modest.

V. DISCUSSION

The features of the NWDOS curves for Mg_{0.75}Al_{0.25}B₂ (Fig. 2) shift systematically to lower energies with temperature, consistent with a quasiharmonic model. The difference spectra of Fig. 10 for Mg_{0.75}Al_{0.25}B₂ show the characteristics of peak broadenings and shifts to lower energies, where there is increased intensity on the low-energy side of a peak and a sharper loss of intensity on the high-energy side. The prominent changes in the difference spectra of MgB₂ from 80 to 100 meV increase monotonically with temperature.

The high sensitivity of the E_{2g} modes to relatively small amounts of Al concentration in Mg-rich alloys is understood as an effect of electronic structure on interatomic forces. We have some evidence that temperature plays a similar role. Our theoretical calculations on MgB₂ based on the quasiharmonic model (Fig. 5) show that all features in the phonon DOS

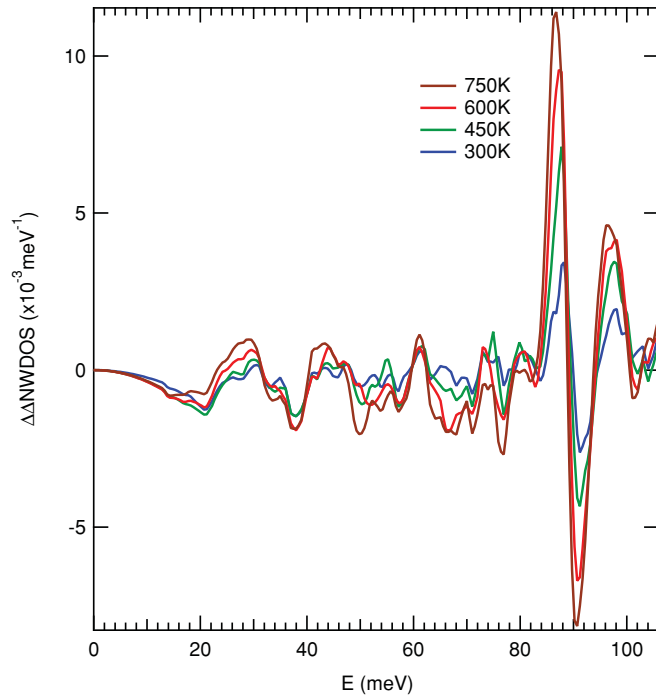


FIG. 7. (Color online) Difference between Δ NWDOS (Experiment, Fig. 6) and Δ NWDOS (Theory, Fig. 6) at temperatures as labeled.

soften monotonically with temperature. The differences of experimental spectra (Fig. 6) show less consistency with the computed quasi-harmonic results or with the linearly scaled and broadened NWDOSs. Some differences, such as the narrow peaks from 80 to 100 meV, originate primarily with the sharpness of the peaks in the calculated DOS. In the energy range from 60 to 80 meV, however, the extra intensity in the experimental difference curve requires some modes moving down into this energy range from above, and

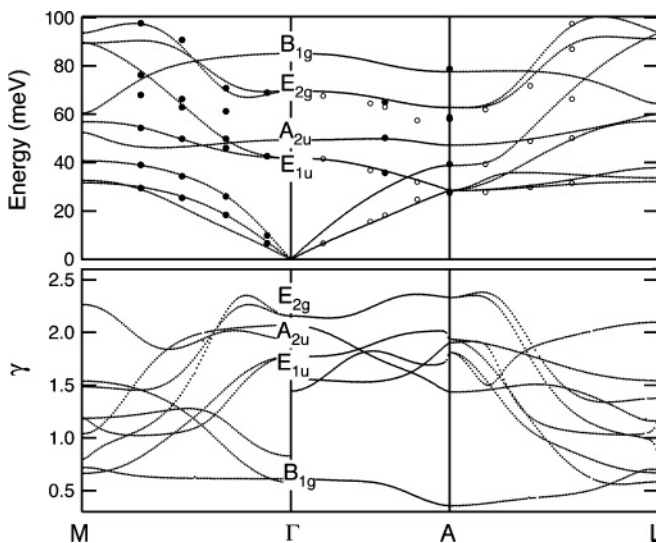


FIG. 8. Upper panel: MgB₂ calculated phonon dispersions compared with experimental results from Ref. 20 (filled circles) and Ref. 14 (open circles). Bottom panel: Calculated dispersions of Grüneisen parameter γ .

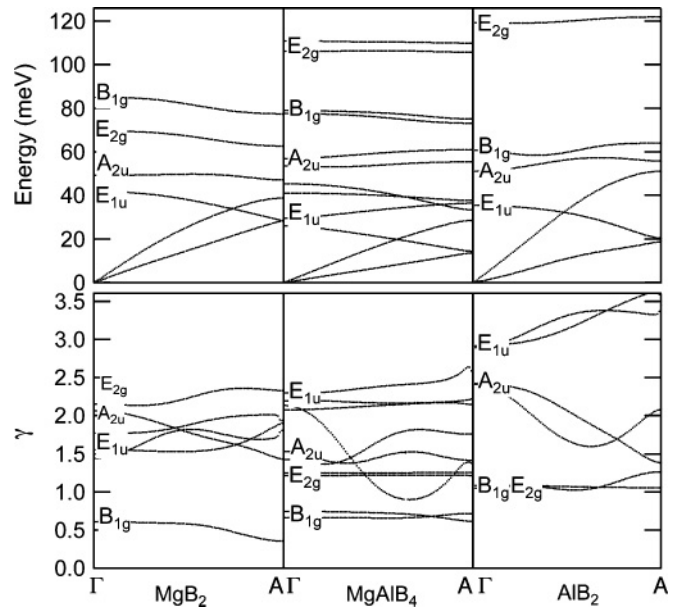


FIG. 9. Comparison of calculated dispersions (upper panel) and Grüneisen parameters γ along Γ -A direction.

perhaps up from below. Unlike in the calculated results, the temperature dependence of the experimental difference spectra from 60 to 80 meV is different for MgB₂ and Mg_{0.75}Al_{0.25}B₂ (Fig. 10). Compared to the low-temperature NWDOS, the NWDOS of MgB₂ shows relatively little change at 450 K, but differs strongly at 600 and 750 K. The difference spectra

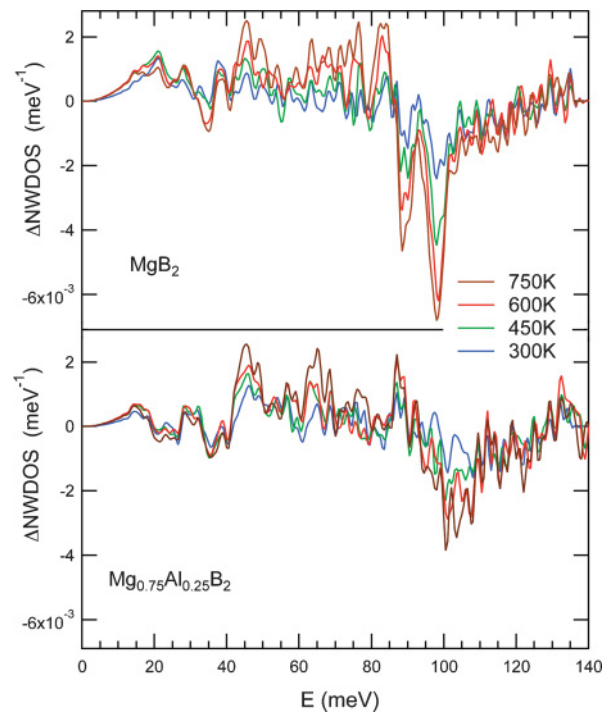


FIG. 10. (Color online) Difference spectra of NWDOSs of MgB₂ and Mg_{0.75}Al_{0.25}B₂ in the 300–750 K temperature range. The experimental curves were corrected for the differences between the spectra acquired from samples in the furnace and refrigerator at 300 K.

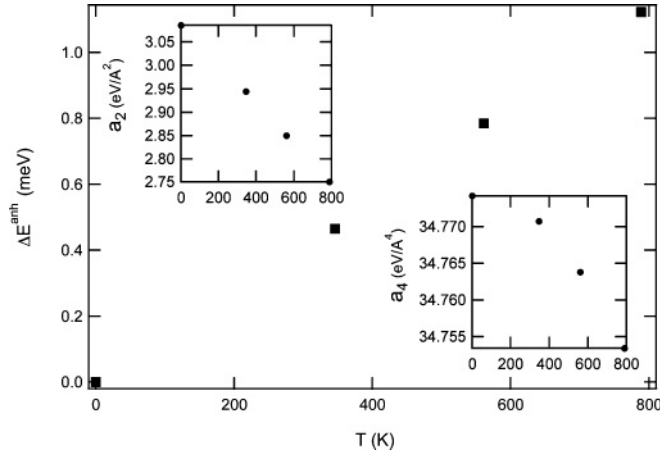


FIG. 11. Shift of $E^{\text{anh}} = E^{\text{tot}} - E^{\text{QH}}$ for E_{2g} mode relative to 0 K value, $\Delta E^{\text{anh}} = E^{\text{anh}}(T) - E^{\text{anh}}(0 \text{ K})$. Insets display the variation of the fitting parameters for the E_{2g} potential surface.

of $\text{Mg}_{0.75}\text{Al}_{0.25}\text{B}_2$ are more monotonic with temperature. These effects are small, but are larger than the variations of the measured spectra. The energy range of 60 to 80 meV includes the E_{2g} boron modes along Γ -A, which have strong electron-phonon coupling. It is possible that some phonon softening from the adiabatic electron-phonon coupling is lost as the electron DOS near the Fermi level is broadened with temperature. The temperature range for this change seems to be between 500 and 600 K, above which a monotonic change is seen again in the difference spectra of MgB_2 . Concerning the large broadening of the peak at 95 meV (Fig. 1), there is an evidence¹⁴ that the third order anharmonicity of the E_{2g} mode is sensitive to temperature and could perhaps be responsible for the broadening.

To understand the possible role of anharmonicity from phonon-phonon interactions, we calculated the behavior of a single E_{2g} mode, which does not contain third-order anharmonicity.^{9,15,22} The calculations were performed with the frozen-phonon approximation at the Γ point.^{6,7,9,13,15,22} This approximation is reported to heavily overestimate the absolute value of the frequency shift,²³ but we are interested in its relative change with temperature. At each lattice expansion obtained from the QH model, we generated the potential surface along the effective coordinate of the mode, u , and fitted it with the potential to a polynomial of form $a_2 u^2 + a_4 u^4$. The phonon energies E_{tot} were computed by solving the secular problem. We obtain an anharmonic phonon energy shift of 9.24 meV at 0 K, in good agreement with 9.46 meV from previous work.²³ A measure of anharmonicity is the ratio of the quartic to the squared quadratic coefficient, $a_4/a_2^2 = 3.6 \text{ eV}^{-1}$. This is on the lower bound of 4–8 eV^{-1} from

Refs. 9 and 15. Figure 11 shows that the anharmonic energy shift increases slowly with temperature. At 0.46 meV at 300 K, it is smaller than a previous report of 1.22 meV,²³ using experimental lattice parameters at 0 and 300 K. Using fourth-order phonon-phonon perturbation theory, the same authors obtained 0.38 meV. At 750 K, our frozen-phonon model gives an anharmonic phonon energy shift of 0.66 meV. This could account for some of the nonquasiharmonic effects seen in the NWDOS of MgB_2 at high temperatures, but these anharmonic effects are small and without the third-order anharmonicity they may be overestimated. Furthermore, they are monotonic with temperature, so it seems most likely that the effects of temperature on phonons in the energy range of 60 to 80 meV originate with the temperature dependence of the EPI.

VI. CONCLUSION

Phonon spectra were measured on MgB_2 and $\text{Mg}_{0.75}\text{Al}_{0.25}\text{B}_2$ at temperatures from 7 to 750 K, showing a broadening and general softening of the phonon DOS. The average behavior can be explained by the quasiharmonic model, where a free energy is obtained for a solid that expands because its lower phonon entropy counteracts the energy cost of expansion. *Ab initio* free-energy calculations were performed to predict the phonon softening in the quasiharmonic model, and were generally successful for MgB_2 . Significant thermal broadenings of the phonons in MgB_2 were observed, however, inconsistent with the quasiharmonic approximation. A frozen-phonon calculation performed at the Γ point gave small effects from phonon anharmonicity that increase the phonon energy with temperature. These quasiharmonic and anharmonic effects are monotonic with temperature, and the neutron-weighted phonon DOS of MgB_2 showed a nonmonotonic behavior between 425 and 600 K that may be related to a change with temperature in the electron-phonon interaction. The effect is small, however, and difficult to discern from the measured spectra. Neither the phonon-phonon anharmonicity nor the electron-phonon interaction makes a substantial contribution to the vibrational entropy of MgB_2 .

ACKNOWLEDGMENTS

This work was supported by the Department of Energy through the Basic Energy Sciences Grant No. DE-FG02-03ER46055. The portions of this work conducted at Oak Ridge National Laboratory were supported by the Scientific User Facilities Division and by the Division of Materials Sciences and Engineering, Office of Basic Energy Sciences, DOE. This work benefited from DANSE software developed under NSF Grant No. DMR-0520547.

¹J. Nagamatsu, N. Nakagawa, T. Muranaka, Y. Zenitani, and J. Akimitsu, *Nature (London)* **410**, 63 (2001).

²C. Buzea and T. Yamashita, *Supercond. Sci. Technol.* **14**, R115 (2001).

³S. L. Bud'ko, G. Lapertot, C. Petrovic, C. E. Cunningham, N. Anderson, and P. C. Canfield, *Phys. Rev. Lett.* **86**, 1877 (2001).

⁴H. Choi, D. Roundy, H. Sun, M. Cohen, and S. Louie, *Nature (London)* **418**, 758 (2002).

- ⁵S. Tsuda, T. Yokoya, Y. Takano, H. Kito, A. Matsushita, F. Yin, J. Itoh, H. Harima, and S. Shin, *Phys. Rev. Lett.* **91**, 127001 (2003).
- ⁶A. Y. Liu, I. I. Mazin, and J. Kortus, *Phys. Rev. Lett.* **87**, 087005 (2001).
- ⁷J. Kortus, I. I. Mazin, K. D. Belashchenko, V. P. Antropov, and L. L. Boyer, *Phys. Rev. Lett.* **86**, 4656 (2001).
- ⁸Y. Kong, O. V. Dolgov, O. Jepsen, and O. K. Andersen, *Phys. Rev. B* **64**, 020501 (2001).
- ⁹T. Yildirim, O. Gülseren, J. W. Lynn, C. M. Brown, T. J. Udovic, Q. Huang, N. Rogado, K. A. Regan, M. A. Hayward, J. S. Slusky, T. He, M. K. Haas, P. Khalifah, K. Inumaru, and R. J. Cava, *Phys. Rev. Lett.* **87**, 037001 (2001).
- ¹⁰J. M. An and W. E. Pickett, *Phys. Rev. Lett.* **86**, 4366 (2001).
- ¹¹P. P. Singh, *Phys. Rev. Lett.* **87**, 087004 (2001).
- ¹²K. P. Bohnen, R. Heid, and B. Renker, *Phys. Rev. Lett.* **86**, 5771 (2001).
- ¹³H. J. Choi, D. Roundy, H. Sun, M. L. Cohen, and S. G. Louie, *Phys. Rev. B* **66**, 020513 (2002).
- ¹⁴A. Shukla, M. Calandra, M. d'Astuto, M. Lazzeri, F. Mauri, C. Bellin, M. Krisch, J. Karpinski, S. M. Kazakov, J. Jun, D. Daghero, and K. Parlinski, *Phys. Rev. Lett.* **90**, 095506 (2003).
- ¹⁵K. Kunc, I. Loa, K. Syassen, R. K. Kremer, and K. Ahn, *J. Phys.: Condens. Matter* **13**, 9945 (2001).
- ¹⁶J. Hlinka, I. Gregora, J. Pokorný, A. Plecenik, P. Kus, L. Satrapinsky, and S. Benacka, *Phys. Rev. B* **64**, 140503 (2001).
- ¹⁷X. K. Chen, M. J. Konstantinović, J. C. Irwin, D. D. Lawrie, and J. P. Franck, *Phys. Rev. Lett.* **87**, 157002 (2001).
- ¹⁸L. Shi, H. Zhang, L. Chen, and Y. Feng, *J. Phys.: Condens. Matter* **16**, 6541 (2004).
- ¹⁹D. Di Castro, E. Cappelluti, M. Lavagnini, A. Sacchetti, A. Palenzona, M. Putti, and P. Postorino, *Phys. Rev. B* **74**, 100505 (2006).
- ²⁰M. d'Astuto, M. Calandra, S. Reich, A. Shukla, M. Lazzeri, F. Mauri, J. Karpinski, N. D. Zhigadlo, A. Bossak, and M. Krisch, *Phys. Rev. B* **75**, 174508 (2007).
- ²¹A. Mialitsin, B. S. Dennis, N. D. Zhigadlo, J. Karpinski, and G. Blumberg, *Phys. Rev. B* **75**, 020509 (2007).
- ²²L. Boeri, G. B. Bachelet, E. Cappelluti, and L. Pietronero, *Phys. Rev. B* **65**, 214501 (2002).
- ²³M. Lazzeri, M. Calandra, and F. Mauri, *Phys. Rev. B* **68**, 220509 (2003).
- ²⁴D. Hinks, H. Claus, and J. Jorgensen, *Nature (London)* **411**, 457 (2001).
- ²⁵A. Q. R. Baron, H. Uchiyama, Y. Tanaka, S. Tsutsui, D. Ishikawa, S. Lee, R. Heid, K.-P. Bohnen, S. Tajima, and T. Ishikawa, *Phys. Rev. Lett.* **92**, 197004 (2004).
- ²⁶V. Y. Tarenkov, A. I. D'yachenko, S. L. Sidorov, V. A. Boichenko, D. I. Boichenko, S. Chromik, V. Strbik, S. Gazi, M. Spankova, and S. Benacka, *Phys. Solid State* **51**, 1778 (2009).
- ²⁷M. Calandra and F. Mauri, *Phys. Rev. B* **71**, 064501 (2005).
- ²⁸E. Cappelluti, *Phys. Rev. B* **73**, 140505 (2006).
- ²⁹A. M. Saitta, M. Lazzeri, M. Calandra, and F. Mauri, *Phys. Rev. Lett.* **100**, 226401 (2008).
- ³⁰O. Delaire, M. S. Lucas, J. A. Muñoz, M. Kresch, and B. Fultz, *Phys. Rev. Lett.* **101**, 105504 (2008).
- ³¹O. Delaire, M. G. Kresch, J. A. Muñoz, M. S. Lucas, J. Y. Y. Lin, and B. Fultz, *Phys. Rev. B* **77**, 214112 (2008).
- ³²B. Fultz, *Prog. Mater. Sci.* **55**, 247 (2010).
- ³³R. Osborn, E. A. Goremychkin, A. I. Kolesnikov, and D. G. Hinks, *Phys. Rev. Lett.* **87**, 017005 (2001).
- ³⁴J. D. Jorgensen, D. G. Hinks, and S. Short, *Phys. Rev. B* **63**, 224522 (2001).
- ³⁵H. Birkedal, W. Van Beek, H. Emerich, and P. Pattison, *J. Mater. Sci. Lett.* **22**, 1069 (2003).
- ³⁶R. Lortz, C. Meingast, D. Ernst, B. Renker, D. Lawrie, and J. Franck, *J. Low Temp. Phys.* **131**, 1101 (2003).
- ³⁷Y. Xue, S. Asada, A. Hosomichi, S. Naher, J. Xue, H. Kaneko, H. Suzuki, T. Muranaka, and J. Akimitsu, *J. Low Temp. Phys.* **138**, 1105 (2005).
- ³⁸J. J. Neumeier, T. Tomita, M. Debessai, J. S. Schilling, P. W. Barnes, D. G. Hinks, and J. D. Jorgensen, *Phys. Rev. B* **72**, 220505 (2005).
- ³⁹X. Wan, J. Dong, H. Weng, and D. Y. Xing, *Phys. Rev. B* **65**, 012502 (2001).
- ⁴⁰B. Renker, K. B. Bohnen, R. Heid, D. Ernst, H. Schober, M. Koza, P. Adelman, P. Schweiss, and T. Wolf, *Phys. Rev. Lett.* **88**, 067001 (2002).
- ⁴¹M. Kresch, O. Delaire, R. Stevens, J. Y. Y. Lin, and B. Fultz, *Phys. Rev. B* **75**, 104301 (2007).
- ⁴²M. Kresch, M. Lucas, O. Delaire, J. Y. Y. Lin, and B. Fultz, *Phys. Rev. B* **77**, 024301 (2008).
- ⁴³P. Giannozzi, S. Baroni, N. Bonini, M. Calandra, R. Car, C. Cavazzoni, D. Ceresoli, G. L. Chiarotti, M. Cococcioni, I. Dabo, A. D. Corso, S. de Gironcoli, S. Fabris, G. Fratesi, R. Gebauer, U. Gerstmann, C. Gougoussis, A. Kokalj, M. Lazzeri, L. Martin-Samos, N. Marzari, F. Mauri, R. Mazzarello, S. Paolini, A. Pasquarello, L. Paulatto, C. Sbraccia, S. Scandolo, G. Scaluzero, A. P. Seitsonen, A. Smogunov, P. Umari, and R. M. Wentzcovitch, *J. Phys.: Condens. Matter* **21**, 395502 (2009).
- ⁴⁴J. P. Perdew, K. Burke, and M. Ernzerhof, *Phys. Rev. Lett.* **77**, 3865 (1996).
- ⁴⁵D. Vanderbilt, *Phys. Rev. B* **41**, 7892 (1990).
- ⁴⁶N. Troullier and J. L. Martins, *Phys. Rev. B* **43**, 1993 (1991).
- ⁴⁷H. J. Monkhorst and J. D. Pack, *Phys. Rev. B* **13**, 5188 (1976).
- ⁴⁸M. Methfessel and A. T. Paxton, *Phys. Rev. B* **40**, 3616 (1989).
- ⁴⁹U. Burkhardt, V. Gurin, F. Haarmann, H. Borrmann, W. Schnelle, A. Yaresko, and Y. Grin, *J. Solid State Chem.* **177**, 389 (2004).
- ⁵⁰S. Margadonna, K. Prassides, I. Arvanitidis, M. Pissas, G. Papavasiliou, and A. N. Fitch, *Phys. Rev. B* **66**, 014518 (2002).
- ⁵¹P. Giannozzi, S. de Gironcoli, P. Pavone, and S. Baroni, *Phys. Rev. B* **43**, 7231 (1991).
- ⁵²B. Grabowski, L. Ismer, T. Hickel, and J. Neugebauer, *Phys. Rev. B* **79**, 134106 (2009).